Journal of Applied Mechanics and Technical Physics, Vol. 45, No. 2, pp. 187–198, 2004

ONE SINGULARLY PERTURBED PROBLEM OF TURBULENT GAS DYNAMICS

A. V. Omel'chenko and É. A. Tropp

UDC 533.6.011.72

The problem of the interaction of a Prandtl–Mayer wave with a shear layer is solved using the small parameter method for the case where the flow vorticity in the shear layer is small. A direct expansion is constructed and its inadequacy at large distances from the vortex layer is proved. The strained coordinate method is used to obtain a uniformly adequate expansion. It is shown that for certain velocity distributions in the shear layer, the characteristics in the reflected simple wave resulting from the interaction intersect each other and a shock arises in the flow. There coordinates of the shock origin and the function describing the shock shape are obtained.

Key words: *simple-wave interaction, gas dynamics, asymptotic expansions, singular problem.*

Introduction. The interaction of a simple wave with a shear layer is encountered in descriptions of supersonic jet flows [1, 2], interactions of shocks with simple waves [3, 4], and in problems of exterior aerodynamics [5, 6]. From the viewpoint of wave classification, a shear layer is a degenerate simple wave [7]; therefore, the problem at hand is a problem of simple-wave interaction.

Traditionally, the interaction of simple waves has been studied with the use of group analysis [7–9]. However, exact analytical solutions of such problems are possible only in exclusive cases — an exact solution cannot be obtained even to the problem of the interaction of Prandtl–Mayer simple waves [7]. In this connection, of great significance are approximate methods for solving similar problems, the main of which is asymptotic small-parameter expansion [10, 11].

The small-parameter method has been used to solve the problem of simple-wave interaction in many papers (see, e.g., [11–18]). In most of them, the flow was considered isentropic and the trivial solution $u = \text{const}$ was used as the zero approximation.

In the problem considered, the small parameter is the flow vorticity in the shear layer. In the zero approximation, a simple wave solution is used. The unboundedness of the interaction region is responsible for the nonuniformity the direct expansion. A uniformly adequate expansion is constructed using the strained coordinate method [10, 11].

1. Formulation of the Problem. The interaction of an isentropic centered rarefaction wave 1 with a vortex (shear) layer 2 of finite thickness (see Fig. 1) is considered using the ideal perfect gas model. The flow in the interaction region is described by the Euler equations. It is convenient to pass from this system to the extended system [19]; for the case of a planar supersonic flow, it has the form

$$\frac{dP_{1,2}}{d\nu_{1,2}} = \pm\frac{\psi}{\cos^2(\vartheta \pm \alpha)}\,[-\mathrm{M}^2 P_{1,2}^2 - (2\mu - \mathrm{M}^2)P_1P_2 + 2\mu P_{1,2}P_3]$$

$$\pm Z\Big[-\frac{2P_1P_2\cos\alpha}{\cos(\vartheta-\alpha)\cos(\vartheta+\alpha)} + \frac{P_1P_3}{\cos(\vartheta+\alpha)\cos\vartheta} + \frac{P_2P_3}{\cos(\vartheta-\alpha)\cos\vartheta}\Big],$$

$$\frac{dP_3}{d\nu_3} = \frac{P_3}{2\Gamma(\mathrm{M})\cos^2\vartheta}\,(P_2 - P_1), \qquad \Gamma(\mathrm{M}) = \frac{\gamma\mathrm{M}^2}{A}, \tag{1.1}$$

St. Petersburg State Polytechnical University, St. Petersburg 195251. Translated from Prikladnaya Mekhanika i Tekhnicheskaya Fizika, Vol. 45, No. 2, pp. 47–61, March–April, 2004. Original article submitted October 24, 2003.

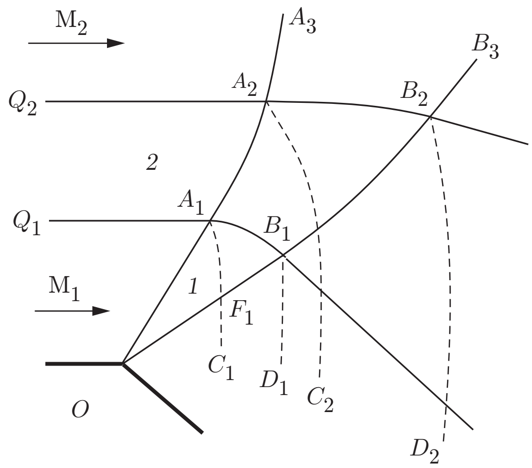

Fig. 1. Diagram of interaction of a centered rarefaction wave with a vortex layer.

$$\frac{\partial\vartheta}{\partial x} = \frac{P_2\tan(\vartheta-\alpha) - P_1\tan(\vartheta+\alpha)}{2\Gamma(\mathrm{M})}, \qquad \frac{\partial\vartheta}{\partial y} = \frac{P_1 - P_2}{2\Gamma(\mathrm{M})},$$

$$\frac{\partial \mathrm{M}}{\partial x} = \nu\Big[-P_3\tan\vartheta + \frac{P_2\tan(\vartheta-\alpha) - P_1\tan(\vartheta+\alpha)}{2}\Big], \quad \frac{\partial \mathrm{M}}{\partial y} = \nu\Big[P_3 - \frac{P_1+P_2}{2}\Big], \qquad \nu = \frac{\mu}{(1+\varepsilon)\mathrm{M}}.$$

Here M is the Mach number, ϑ is the slope of the velocity vector to the abscissa, $\alpha = \arcsin(1/\mathrm{M})$, and γ is the adiabatic exponent;

$$Z = \frac{\mathrm{M}^2-2}{2A^2}\,\frac{\mu}{(1+\varepsilon)\mathrm{M}^3}; \quad \psi = \frac{1}{2(1+\varepsilon)\mathrm{M}^2 A}; \quad \mu = 1+\varepsilon A^2; \qquad A = \sqrt{\mathrm{M}^2-1}; \qquad \varepsilon = (\gamma-1)/(\gamma+1).$$

In (1.1), the functions

$$P_{1,2} = \frac{\partial \ln p}{\partial y} \pm \Gamma(\mathrm{M})\,\frac{\partial\vartheta}{\partial y}, \qquad P_3 = \frac{\partial \ln p}{\partial y} + \frac{(1+\varepsilon)\mathrm{M}^2}{\mu}\,\frac{\partial \ln \mathrm{M}}{\partial y}$$

characterize the intensity of the small perturbations propagating along the characteristics of the first (P_1) and second (P_2) families and along the streamlines (P_3). Thus, in the simple Prandtl–Mayer wave, $P_2 = P_3 = 0$, and

$$P_1 = \frac{2(1+\varepsilon)\sqrt{\mathrm{M}^2-1}\cos^2(\vartheta+\alpha)}{x-c}. \tag{1.2}$$

The constant c changes in passage from one characteristic of the first family to another. In the centered wave, this quantity is constant throughout the wave and is equal to the abscissa x_0 of the center (x_0, y_0) of the wave.

In addition, from (1.1) it follows that

$$\frac{d\vartheta}{d\nu_3} + \frac{(1-\varepsilon)\sqrt{\mathrm{M}^2-1}}{\mu}\,\frac{d\ln\mathrm{M}}{d\nu_3} = \frac{d\vartheta}{d\nu_3} + \frac{d\omega(\mathrm{M})}{d\nu_3} = 0,$$

where $\omega(\mathrm{M})$ is the function calculated by the formula

$$\omega(\mathrm{M}) = (1/\sqrt{\varepsilon})\arctan\sqrt{\varepsilon(\mathrm{M}^2-1)} - \arctan\sqrt{\mathrm{M}^2-1}.$$

Hence, throughout the wave, the following relation is valid:

$$\vartheta + \omega(\mathrm{M}) = \vartheta_1 + \omega(\mathrm{M}_1). \tag{1.3}$$

Here ϑ_1 and M_1 are the values of these variables on an arbitrary characteristic of the first family.

For the centered wave, it is convenient to convert to polar coordinates (r, φ) with origin at the center of the wave. In this coordinate system, the polar angle φ is linked to the Mach number M and the slop ϑ of the streamline in the wave by the relation

$$\varphi = \vartheta + \alpha = \vartheta + \arcsin(1/\mathrm{M}) = \vartheta_1 + \omega(\mathrm{M}_1) - \omega(\mathrm{M}) + \arcsin(1/\mathrm{M}),$$

which, in view of the equality

$$\arcsin(1/\mathrm{M}) + \arctan\sqrt{\mathrm{M}^2 - 1} = \pi/2$$

can be written as

$$\varphi = -\tilde{\omega}(\mathrm{M}) + C_1, \qquad \tilde{\omega}(\mathrm{M}) = (1/\sqrt{\varepsilon}\,)\arctan\sqrt{\varepsilon(\mathrm{M}^2 - 1)},$$
$$C_1 = \vartheta_1 + \arcsin(1/\mathrm{M}_1) + \tilde{\omega}(\mathrm{M}_1) = \varphi_1 + \tilde{\omega}(\mathrm{M}_1). \tag{1.4}$$

Solving (1.4) for the Mach number, we obtain the explicit form of the function $\mathrm{M}(\varphi)$ in the centered wave:

$$\mathrm{M}(\varphi) = \sqrt{(1/\varepsilon)\tan(\sqrt{\varepsilon}\,[C_1 - \varphi])^2 + 1}. \tag{1.5}$$

Using the dependence (1.5), it is east to write the functions $r_l(\varphi)$ and $r_h(\varphi)$ describing the streamline shape and the characteristics of the second family in the centered wave. Indeed, from geometrical reasons it follows that

$$\frac{r_l d\varphi}{dr_l} = -\cot\alpha = -A, \qquad \frac{r_h d\varphi}{dr_h} = -\cot 2\alpha = -\frac{A^2 - 1}{2A}, \qquad A := \sqrt{\mathrm{M}^2 - 1}.$$

Integration of these equalities yields the following expressions for the streamline and the characteristic of the second family that passes through the point with the coordinates (r_1, φ_1):

$$r_l(\varphi) = r_1\Big[\frac{\mu(\mathrm{M}(\varphi))}{\mu(\mathrm{M}(\varphi_1))}\Big]^{1/2\varepsilon}, \qquad r_h(\varphi) = r_1\frac{R(\mathrm{M})}{R(\mathrm{M}_1)}, \qquad R(\mathrm{M}) = \sqrt{\frac{\mu^{æ}}{A}}. \tag{1.6}$$

The shear layer 2, in which $P_3 \neq 0$ and $P_1 = P_2 = 0$, is a degenerate simple wave, according to the classification of [8]. Indeed, as can be seen from (1.1), the conditions $P_1 = P_2 = 0$ imply that in this wave $p = \mathrm{const}$ and $\vartheta = \mathrm{const}$, i.e., this wave represents isobaric motion in which all characteristics of the third kind (streamlines) are straight lines parallel to one another. Because the derivatives $d\ln\mathrm{M}/d\nu_3$ and $dP_3/d\nu_3$ are equal to zero in this wave, the functions P_3 and M do not vary along the streamlines.

Let us introduce Cartesian coordinates with origin at the point O and the x axis parallel to the streamlines of the incoming flow. In this case, the equality $dP_3/d\nu_3 = 0$ implies that the functions P_3 and M in the shear layer depend only on y and are related by the formula

$$P_3(y) = \frac{(1+\varepsilon)\mathrm{M}^2(y)}{\mu(y)}\frac{d\ln\mathrm{M}(y)}{dy} = \frac{d\ln\mu^{æ}(y)}{dy}, \tag{1.7}$$

which allows one to determine the function $\mu(y)$ from the given $P_3 = P_3(y)$:

$$\mu(y) = \mu(y_1)\exp\int\limits_{y_1}^{y} P_3(y)\,dy.$$

Let us describe the interaction of the centered Prandtl–Mayer wave 1 with the shear layer 2 (see Fig. 1). Before the interaction, the shear layer 2, bounded by the weak tangential discontinuities Q_1A_1 and Q_2A_2, moves parallel to the wall. At the point O, a break of the surface occurs, resulting in the centered Prandtl–Mayer wave 1 bounded by the weak discontinuities OA_1 and OB_1.

The intersection of the weak discontinuity OA_3 with the weak horizontal discontinuities Q_1A_1 and Q_2A_2 leads to the formation of the outgoing weak discontinuities A_1C_1 and A_2C_2, respectively. At the points B_1 and B_2, the weak horizontal discontinuities A_1B_1 and A_2B_2 intersect the weak discontinuity OB_1B_2 closing the Prandtl–Mayer wave, leading to the formation of the weak discontinuities B_1D_1 and B_2D_2. Thus, on the left, the interaction region is bounded by the weak discontinuity OA_3, which is a continuation of the weak discontinuity OA_1 separating the uniform flow and the Prandtl–Mayer wave; from below, the interaction region is bounded by the weak discontinuity $A_1F_1C_1$ issuing from the point A_1 of intersection of the weak discontinuities OA_1 and Q_1A_1.

Along the characteristic OA_3, the slope ϑ of the velocity vector to the x axis and the function P_2 are equal to zero and the Mach number distribution depends only on y. On the segments OA_1 and A_2A_3, the function $\mathrm{M}(y)$ is constant and equal to the Mach numbers M_1 and M_2 under and above the shear layer 2, and on the segment A_1A_2, this function is determined by the specified flow vorticity $P_3(y)$ [formula (1.7)]. The shape of the characteristic of the first family OA_3 is easily found from the known function $\mathrm{M}(y)$ using the relation $dy/dx = \tan\alpha(y)$ [$\alpha = \arcsin(1/\mathrm{M})$].

At the weak discontinuity OA_3, the function P_1 has a jump: this function is equal to zero to the left of OA_3 and is different from zero to the right of it. On the segment OA_1 in the coordinate system with origin at the point O, the function P_1 is defined by formula (1.2)

$$P_1 = \frac{2(1+\varepsilon)A(\mathrm{M}_1)\cos^2\alpha(\mathrm{M}_1)}{x} = \frac{2(1+\varepsilon)A^3(\mathrm{M}_1)}{\mathrm{M}_1^2 x},$$

and on the segment A_1A_2, it is described by the first-order partial differential equation resulting from (1.1):

$$\frac{\partial P_1}{\partial x} + \frac{1}{A(\mathrm{M}(y))}\frac{\partial P_1}{\partial y} = a_2(y)P_1^2 + a_1(y)P_1,$$

$$a_1(y) = \frac{\mu(\mathrm{M}(y))(3\mathrm{M}^2(y)-2)P_3(y)}{2(1+\varepsilon)\mathrm{M}^2(y)A^3(\mathrm{M}(y))}, \qquad a_2(y) = -\frac{\mathrm{M}^2(y)}{2(1+\varepsilon)A^3(\mathrm{M}(y))}.$$

The solution of the latter equation has the form

$$P_1(x,y) = \frac{2(1+\varepsilon)\mathrm{M}(y)\sqrt{A(\mathrm{M}(y))}}{\mathrm{M}_1^3 A^{-5/2}(\mathrm{M}_1)(x-F_0(y)) + g(y)},$$

where

$$F_0(y) = \int\limits_{y_0}^{y} A(\mathrm{M}(y))\,dy, \qquad g(y) = \int\limits_{y_0}^{y}\Big[\frac{\mathrm{M}(y)}{\sqrt{A(\mathrm{M}(y))}}\Big]^3 dy$$

[y_0 is the ordinate of the point A_1 (see Fig. 1)]. Because along A_1A_2,

$$x = x_0 + \int\limits_{y_0}^{y} A(\mathrm{M}(y))\,dy = x_0 + F_0(y),$$

then on the characteristic A_1A_2, we have

$$P_1(y) = \frac{2(1+\varepsilon)\mathrm{M}(y)\sqrt{A(\mathrm{M}(y))}}{\mathrm{M}_1^3 A^{-5/2}(\mathrm{M}_1)x_0 + g(y)}.$$

Finally, above the point A_2, the function P_1 is given by the relation

$$P_1 = \frac{2(1+\varepsilon)A^3(\mathrm{M}_2)}{\mathrm{M}_2^2(x+c)}, \qquad c = \frac{2(1+\varepsilon)A^3(\mathrm{M}_2)}{\mathrm{M}_2^2 P_1(x_a)} - x_a,$$

where x_a is the abscissa of the point A_2.

To describe the gas-dynamic functions on the lower boundary $A_1F_1C_1$ of the interaction region, we use a polar coordinate system with origin at the point O. In this system, the shape of the characteristic of the second family A_1F_1 in the wave 1, the distribution of the Mach number $\mathrm{M}(\varphi)$ [formula (1.5)], and the angle ϑ [formula (1.3)] along this characteristic are found from the angle φ from the given range $[\varphi_1, \varphi_2]$, $\varphi_1 = \arcsin(1/\mathrm{M}_1)$ using formula (1.6).

The weak tangential discontinuities A_1B_1 and A_2B_2 issuing from the points A_1 and A_2 separate the region in which $P_3 = 0$ from the region in which $P_3 \neq 0$. However, the latter region is no longer a shear layer because in it, not only the function P_3 but also the functions P_1 and P_2 are different from zero. In the following, this region with variable entropy is called a vortex layer.

The interaction of the vortex layer with the weak discontinuity OB_3 results in an abrupt change in the function P_1. In this case, behind the segment F_1B_1 and behind the characteristic OF_1 closing the simple wave 1, the function P_1 vanishes, and behind the segment B_1B_3, this function is different from zero. Physically, this is explained by the presence of weak perturbations propagating from the region $A_1A_2B_2B_1$ and interacting with the vortex layer located behind B_1B_2. This interaction results in higher-order weak perturbations arising in the vortex region behind B_1B_2 and propagating along the characteristics of the first kind. Since the intensity of these perturbations is characterized by P_1, this function is different from zero above the discontinuous streamline issuing from the point B_1.

Similarly, it is shown that in the region bounded from above by the streamline issuing from the point B_2 and on the left by the characteristic F_1C_1, the function P_2 is different from zero. Thus, the interaction of the wave with the shear layer results in the formation of vortex layer bounded by the streamlines issuing from the points B_1 and B_2, the simple wave bounded on the left and from below by the characteristic B_2B_3 and the streamline issuing from the point B_2, and the simple wave bounded on the left and from above by the characteristic F_1C_1 and the streamline issuing from the point B_1.

The above pattern takes place until the weak discontinuity $A_1F_1C_1$ reaches the rigid wall bounding the flow in question from below. The reflection results in the formation of perturbations propagating along the characteristics of the first family and overtaking the vortex layer. In addition, in the wave $C_1F_1B_1D_1$ both rarefaction and compression of the flow can occur. In the latter case, the occurrence of a shock due to the intersection of neighboring characteristics in the wave is possible.

Generally, the problem of the interaction of a shear layer with a simple wave has no analytical solutions. The main objective of the present study is to construct analytical solutions by asymptotic small-parameter expansion for the case of small flow vorticity in the shear layer.

2. Constructing Direct Expansion. We introduce the parameter

$$\delta = \max_y |\mathrm{M}(y) - \mathrm{M}_1|/\mathrm{M}_1,$$

which characterizes the flow vorticity in the shear layer 2. Assuming that the flow vorticity is small, we shall attempt to construct an analytical solution of the interaction problem by asymptotic expansion of the functions included in (1.1) in the small parameter δ:

$$f = \sum_{k=0}^{\infty} \delta^k f^{(k)}, \qquad \delta \to 0, \quad f \in \{A, \vartheta, P_1, P_2, P_3\}. \tag{2.1}$$

In the zero approximation, system (1.1) describes the flow in the centered Prandtl–Mayer wave, in which $P_2^{(0)} = P_3^{(0)} = 0$, the function $P_1^{(0)}$ is defined by formula (1.2), and $\vartheta^{(0)}$ and $\mathrm{M}^{(0)}$ are linked to the Mach number M_1 in the uniform flow before the wave 1 and to the polar angle φ by relations (1.5) and (1.3), respectively.

To obtain the first approximation, we shall convert to polar coordinates in system (1.1), substitute series (2.1) into (1.1), and retain terms at δ^1. As a result, for the functions $f^{(1)}$, we obtain

$$\begin{gathered}
\frac{\partial P_3^{(1)}}{\partial \varphi} - r\cot\,(\varphi - \vartheta^{(0)})\frac{\partial P_3^{(1)}}{\partial r} = \alpha_{13}(\varphi)P_3^{(1)},\\
\frac{\partial P_2^{(1)}}{\partial \varphi} - r\cot\,(\varphi + \alpha^{(0)} - \vartheta^{(0)})\,\frac{\partial P_2^{(1)}}{\partial r} = \alpha_{22}(\varphi)P_2^{(1)} + \alpha_{23}(\varphi)P_3^{(1)},\\
\frac{D^{(1)}}{r} + \frac{1}{\nu(\varphi)}\,\frac{\partial \vartheta^{(1)}}{\partial r} = -\alpha_{32}(\varphi)P_2^{(1)}, \qquad D^{(1)} = \vartheta^{(1)} - \frac{A^{(1)}}{(\mathrm{M}^{(0)})^2},\\
\frac{D^{(1)}}{r} + \frac{1}{\mu(\varphi)}\,\frac{\partial A^{(1)}}{\partial r} = \alpha_{32}(\varphi)P_2^{(1)} + \alpha_{33}(\varphi)P_3^{(1)},\\
\frac{D^{(1)}}{r}\,\frac{\partial P_1^{(0)}}{\partial \varphi} + \frac{\partial P_1^{(1)}}{\partial r} = \alpha_{41}(\varphi) + \alpha_{42}(\varphi)P_2^{(1)} + \alpha_{43}(\varphi)P_3^{(1)} + \alpha_{44}(\varphi)\vartheta^{(1)} + \alpha_{45}(\varphi)A^{(1)}.
\end{gathered} \tag{2.2}$$

As the initial system (1.1), system (2.2) is written in invariants [19]. In addition, the matrix of the right side of (2.2) is triangular. These circumstances allow us to obtain an analytical solution of system (2.2) by sequentially solving the inhomogeneous linear first-order partial differential equation included in it for the functions $P_3^{(1)}$, $P_2^{(1)}$, $\vartheta^{(1)}$, $A^{(1)}$, and $P_1^{(1)}$.

Indeed, in the centered wave, the Mach number $\mathrm{M}^{(0)}$ and the angle $\vartheta^{(0)}$ are uniquely expressed in terms of the polar angle φ. Therefore, the first equation of system (2.2) can be written as

$$\frac{\partial P_3^{(1)}}{\partial \varphi} + ra(\varphi)\,\frac{\partial P_3^{(1)}}{\partial r} = P_3^{(1)}F(\varphi). \tag{2.3}$$

For (2.3), the following Cauchy problem is formulated: to find the surface passing through the curve

$$\varphi = \varphi_0, \qquad P_3^{(1)} = f(r).$$

The solution of this problem can be written in explicit form:

$$P_3^{(1)} = \Psi(\varphi) f\Big(\frac{r}{B(\varphi)}\Big), \quad B(\varphi) = \exp\int\limits_{\varphi_0}^{\varphi} a(\varphi)\, d\varphi, \quad \Psi(\varphi) = \exp\int\limits_{\varphi_0}^{\varphi} F(\varphi)\, d\varphi. \tag{2.4}$$

The known form of the function $P_3^{(1)}$ allows us to obtain an analytical expression for $P_2^{(1)}$. Using the notation $z = P_2^{(1)}$, $b(\varphi) = -\cot\,(\varphi + \alpha^{(0)} - \vartheta^{(0)})$, for the second equation in (2.2) we write the characteristic system

$$\frac{d\varphi}{1} = \frac{dr}{rb(\varphi)} = \frac{dz}{\alpha_1(\varphi)\, z + \alpha_2(\varphi)\, \Psi(\varphi)\, f(r/B(\varphi))}.$$

One general integral of this system is easy to find:

$$\frac{r}{D(\varphi)} = C_1, \qquad D(\varphi) = \exp\int\limits_{\varphi_0}^{\varphi} b(\varphi)\, d\varphi.$$

To obtain the second integral, it is necessary to solve the equation

$$z' = \alpha_1(\varphi) z + \alpha_2(\varphi)\Psi(\varphi) f(r/B(\varphi)) = \alpha_1(\varphi) z + \alpha_2(\varphi)\Psi(\varphi) f(C_1 D(\varphi)/B(\varphi)).$$

The general solution of the homogeneous equation is written as

$$z_0 = C_0 \exp\int\limits_{\varphi_0}^{\varphi} \alpha_1(\varphi)\, d\varphi =: C_0 A_1(\varphi).$$

We seek a solution in the form $z = C(x) A_1(\varphi)$. It is easy to show that in this case, the function

$$C(x) = \int\limits_{\varphi_0}^{\varphi} \frac{\alpha_2(\varphi)}{A_1(\varphi)} \Psi(\varphi) f\Big(\frac{C_1 D(\varphi)}{B(\varphi)}\Big)\, d\varphi + C_2 =: \Phi(\varphi, C_1) + C_2.$$

Hence, the general solution is given by

$$z = A_1(\varphi)\tilde{g}(\varphi)(r/D(\varphi)) + A_1(\varphi)\Phi(\varphi, r/D(\varphi)).$$

Here $\tilde{g}$ is an arbitrary function of the argument. We are interested in the solution that vanishes for $\varphi = \varphi_0$. Since for such φ, the function $\Phi = 0$ and $A_1(\varphi) = 1$, then $\tilde{g} \equiv 0$. Therefore, the solution of the Cauchy problem has the form

$$z = A_1(\varphi)\Phi(\varphi, r/D(\varphi)). \tag{2.5}$$

Let us now define the functions $A^{(1)}$ and $\vartheta^{(1)}$. It is to show that the third and fourth equations of system (2.2) can be written as

$$A^{(1)} = \mu^{(0)} E(r, \varphi) - \frac{\mu^{(0)}}{\varphi^{(0)}}\vartheta^{(1)}, \qquad \frac{1}{r}\,\vartheta^{(1)} + \frac{\partial\vartheta^{(1)}}{\partial r} = \frac{\tilde{G}(r, \varphi)}{r}.$$

Integration of the last equation from r_0 to r taking into account that $\vartheta^{(1)} = 0$ at $r = r_0$ yields

$$\vartheta^{(1)} = \frac{1}{r}\int\limits_{r_0}^{r} \tilde{G}(r, \varphi)\, dr.$$

We note that in the case of a vortex layer of finite thickness, the functions $P_3^{(1)}$ and $P_2^{(1)}$ vanish at r greater than a certain r_1. It is possible to show that at such r, the expression for the angle $\vartheta^{(1)}$ becomes simpler and takes the form

$$\vartheta^{(1)} = C_1(\varphi)/r + C_2(\varphi).$$

It should be noted that the interaction region is unbounded along r. The last circumstance is the reason for the nonuniformity of the asymptotic expansion obtained. To prove the last assertion, it is necessary to study the system obtained by substituting series (2.1) into (1.1) and retaining terms with δ^2. After integration of this system, terms of the form $D(\varphi)\ln r$, increasing without limit as $r \to \infty$, appear in the expressions for the functions $\vartheta^{(2)}$, $A^{(2)}$, and $P_1^{(2)}$.

3. Constructing a Uniformly Adequate Expansion by the Strained Coordinate Method. To obtain a uniformly adequate first approximation, we use the strained coordinate method [10, 11]. Let us convert from (r, φ) to the strained variables (s, t) using the formulas

$$\varphi = s + \delta\varphi_2(s,t) + \dots, \qquad r = t.$$

This conversion does not change the form of the functions $P_3^{(1)}(s,t)$ and $P_2^{(1)}(s,t)$ — they are still defined by formulas (2.4) and (2.5) in which r and φ are replaced by t and s, respectively. Changes should occur in the expressions for $\vartheta^{(1)}$ and $A^{(1)}$ obtained by expanding these functions along the characteristics of the first family.

Indeed, in the new coordinates the equation for $\vartheta^{(1)}$ is written as

$$\frac{\partial\vartheta^{(1)}}{\partial t} - \frac{\partial\varphi_2}{\partial t}\frac{\partial\vartheta^{(0)}}{\partial s} - \frac{1}{t}\frac{\partial\vartheta^{(0)}}{\partial s}\Big(\varphi_2 - \vartheta^{(1)} + \frac{A^{(1)}}{(\mathrm{M}^{(0)})^2}\Big) = \alpha_{\vartheta 2}(\varphi)P_2^{(1)}.$$

If φ_2 is chosen from the condition

$$\frac{\partial\varphi_2}{\partial t} + \frac{1}{t}\Big(\varphi_2 - \vartheta^{(1)} + \frac{A^{(1)}}{(\mathrm{M}^{(0)})^2}\Big) = 0, \tag{3.1}$$

then the equation for $\vartheta^{(1)}$ takes the form

$$\frac{\partial\vartheta^{(1)}}{\partial t} = -\frac{P_2^{(1)}}{\cos(\vartheta^{(0)} - \alpha^{(0)})}\,\frac{(A^{(0)})^2}{\gamma(\mathrm{M}^{(0)})^4}.$$

As can be seen from the last equality, the function $\vartheta^{(0)} + \delta\,\vartheta^{(1)}$, as a first approximation, remains constant on the rays $s = \mathrm{const}$ at $t > r_1$. In addition, for $s = \varphi_0$, the function $P_2^{(1)} = 0$, so that along the characteristic OA_3, the examined function is identically equal to zero.

Condition (3.1) can be written as

$$\frac{\partial}{\partial t}(t\varphi_2) = \vartheta^{(1)} - \frac{A^{(1)}}{(\mathrm{M}^{(0)})^2} \quad\Longrightarrow\quad \varphi_2(s,t) = \frac{1}{t}\,\tilde{\varphi}(s) + \frac{1}{t}\int\limits_{t_0}^{t}\Big[\vartheta^{(1)} - \frac{A^{(1)}}{(\mathrm{M}^{(0)})^2}\Big]\,dt.$$

Since at $t = t_0$, we have flow in the simple wave with $\varphi = s$, the arbitrary function $\tilde{\varphi}(s)$ in the last equality should be taken identically equal to zero. Then,

$$\varphi = s + \frac{\delta}{t}\int\limits_{t_0}^{t}\Big[\vartheta^{(1)} - \frac{A^{(1)}}{(\mathrm{M}^{(0)})^2}\Big]\,dt + \dots. \tag{3.2}$$

Continuing the expansion, in the next step we obtain the following equation for $\vartheta^{(2)}$:

$$\frac{\partial\vartheta^{(2)}}{\partial t} - \frac{\partial\varphi_3}{\partial t}\frac{\partial\vartheta^{(0)}}{\partial s} - \frac{1}{t}\frac{\partial\vartheta^{(0)}}{\partial s}\Big(\varphi_3 - \vartheta^{(2)} + \frac{A^{(2)}(\mathrm{M}^{(0)})^2 - A^{(0)}A^{(1)}}{(\mathrm{M}^{(0)})^4}\Big) = \dots.$$

It is easy to show that the choice of the function $\varphi_3(s,t)$ such that

$$\frac{\partial}{\partial t}(t\varphi_3) = \vartheta^{(2)} - \frac{A^{(2)}(\mathrm{M}^{(0)})^2 - A^{(0)}A^{(1)}}{(\mathrm{M}^{(0)})^4}$$

provides for the condition of consistency of the function $\vartheta^{(2)}$ on the rays $s = \mathrm{const}$ at $t > r_1$ and the absence of secular summands in the next terms of the expansion.

We note that as in the problem of supersonic flow around a thin profile [10], the lines $s = \mathrm{const}$ can be interpreted physically as characteristics of the first family refined in view of the next approximations. Indeed,

$$\frac{d\varphi}{dr} = \frac{1}{r}\,\tan(\varphi - \vartheta - \alpha).$$

To a first approximation, we have

$$\frac{d\varphi}{dr} = \frac{1}{r}\Big(-\vartheta^{(1)} + \frac{A^{(1)}}{(\mathrm{M}^{(0)})^2}\Big) \quad\Longrightarrow\quad \varphi = \mathrm{const} + \frac{\delta}{r}\int\limits_{r_0}^{r}\Big[\vartheta^{(1)} - \frac{A^{(1)}}{(\mathrm{M}^{(0)})^2}\Big]\,dr.$$

It is obvious that using s as the integration constant, we obtain equality (3.2).

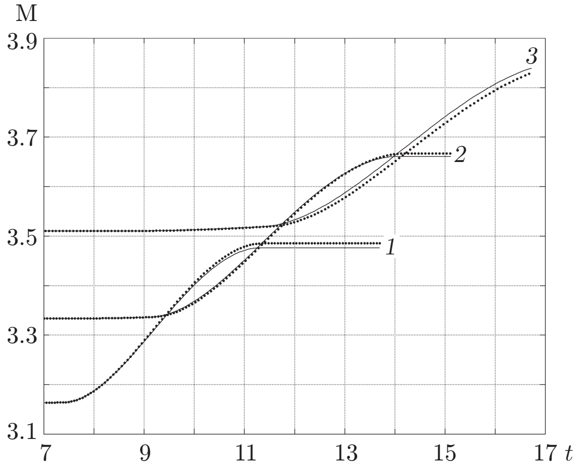

Fig. 2

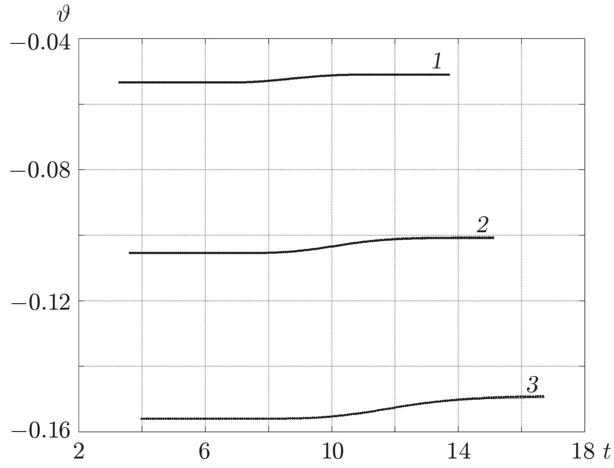

Fig. 3

Fig. 2. Distribution of the Mach number along the characteristics of the first family.

Fig. 3. Distribution of the slope of the velocity vector along the characteristics of the first family.

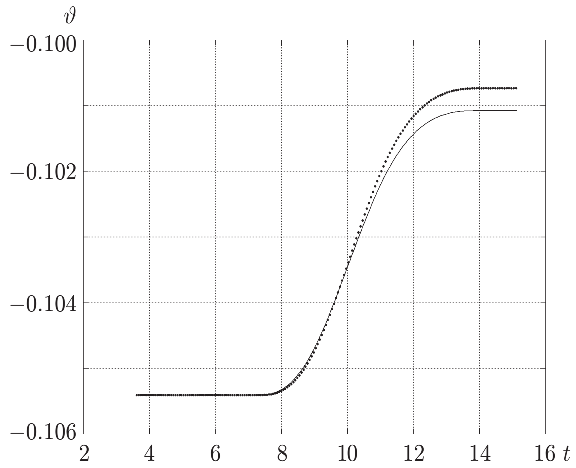

Fig. 4

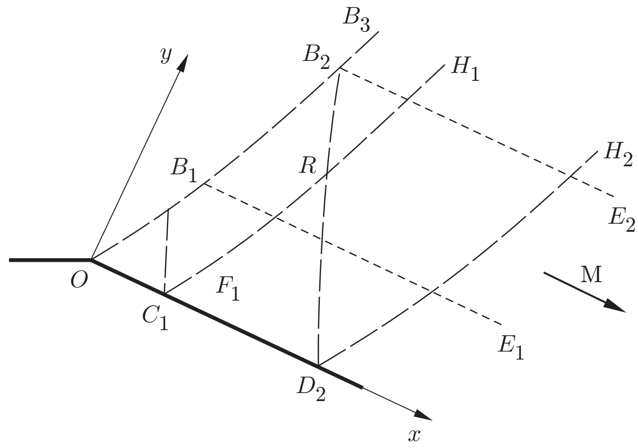

Fig. 5

Fig. 4. Curve of $\vartheta(t)$ for $\mathrm{M}_1 = 3$ and $\mathrm{M}_2 = 3.3$ (comparison of analytical and numerical data).

Fig. 5. Diagram of flow behind the closing characteristic of the centered wave.

Figures 2 and 3 give calculated distributions of the Mach number $\mathrm{M}(t)$ and the angle $\vartheta(t)$ along the characteristics of the first family. The calculations were performed for angles $\vartheta_{w1} = 3$, 6, and 9° (curves 1, 2 and 3, respectively). Before interaction, the Mach number in the shear layer changes smoothly from $\mathrm{M}_1 = 3$ to $\mathrm{M}_2 = 3.3$ ($\delta = 0.1$) under a cubic law. The solid curves correspond to values calculated numerically using the method of characteristics, and the dashed curves, to data obtained using the first two terms of the asymptotic expansion. In Fig. 4, curves 2 from Fig. 3 are scaled up. As is evident from the figures, even the first approximation gives a fairly good fit to the precise calculation — the maximum relative error of the Mach number is about 10^{-4}.

4. Constructing a Solution in the Region behind the Closing Characteristic of the Wave. Behind the last characteristic OB_3 of the wave w_1, there is interaction of the weakly swirled layer $B_1E_1B_2E_2$ with the weakly curved flow in the simple noncentered wave $F_1C_1B_2D_2$ (Fig. 5). The intensity of the vortex layer is characterized by the function P_3, and the intensity of the simple wave is characterized by the function P_2. On the characteristic $F_1B_1B_2$, these functions have order δ, so that

$$P_3P_2 = O(\delta^2), \qquad \delta \to 0.$$

Hence, in the region considered, the flow, to a zero approximation, is a plane-parallel irrotational flow, whose gas-dynamic parameters $\mathrm{M}^{(0)}$ and $\vartheta^{(0)}$ coincide with the Mach number M_{w1} and the angle ϑ_{w1} behind the simple wave w_1. In this case, the functions $P_i^{(0)}$ $(i = 1, 2, 3)$ are equal to zero.

To construct the first approximation, we consider a somewhat more general problem in which all P_i have the same order of smallness of δ, so that

$$P_i P_j = o(P_i) = o(P_j) \qquad \forall\, i, j = 1, 2, 3, \qquad \delta \to 0.$$

In this case, the right sides of Eqs. (1.1) for P_i have order $O(\delta^2)$. Hence, $P_i^{(1)}$ are constant along the characteristics of the ith family. Let us convert to a coordinate system (x, y) with abscissa parallel to the wall (see Fig. 5). In this coordinate system, the general solutions of the equations for $P_i^{(1)}$ have the form

$$P_1^{(1)} = f_1(x - A_{w1}y), \qquad P_2^{(1)} = f_2(x + A_{w1}y), \qquad P_3^{(1)} = f_3(y). \tag{4.1}$$

The functions f_i on the right sides of these relations are determined from the corresponding boundary conditions.

Using expressions (4.1), it is easy to write the general form of the functions $\vartheta^{(1)}$ and $A^{(1)}$:

$$\vartheta^{(1)} = -\frac{1}{2\gamma \mathrm{M}_{w1}^2}\,[F_1(x - A_{w1}y) + F_2(x + A_{w1}y)], \quad A^{(1)} = \frac{\mu_{w1}}{(1+\varepsilon)A_{w1}}\Big[F_3(y) + \frac{F_1(x - A_{w1}y) - F_2(x + A_{w1}y)}{2A_{w1}}\Big],$$

$$F_i = \int\limits_{\xi_{0i}}^{\xi_i} f_i(s)\, ds, \qquad \xi_1 = x - A_{w1}y, \quad \xi_2 = x + A_{w1}y, \quad \xi_3 = y.$$

Reverting to the problem considered, we note that the functions $P_1^{(1)}$, $P_2^{(1)}$, and $P_3^{(1)}$ are different from zero in the regions $C_1H_1D_2H_2$, $F_1C_1B_2D_2$, and $B_1E_1B_2E_2$, respectively. Moreover, the functions $P_2^{(1)}$ and $P_3^{(1)}$, whose values do not change along the characteristics of the second and third families, respectively, are determined from the initial conditions on the segments F_1B_2 and B_1B_2 of the closing characteristic of the wave w_1. In the region $P_1^{(1)}$, the values of the function $C_1H_1D_2H_2$ are determined from the condition that the angle ϑ on the wall is equal to zero:

$$\frac{\partial \vartheta}{\partial x}\Big|_{y=0} = 0 \quad\Longrightarrow\quad P_1^{(1)}(x) = -P_2^{(1)}(x) \quad\Longrightarrow\quad P_1^{(1)}(\xi_1) = -P_2^{(1)}(\xi_2).$$

As a consequence, the function $\vartheta^{(1)}$ is equal to zero in the triangle OF_1C_1 and in the region behind the characteristic D_2H_2, and it is constant along the characteristics of the second and first families in the regions $F_1C_1B_2R$ and $RH_1D_2H_2$, respectively. In the region $B_2B_3RH_1$, this function has a constant value, and in the triangle C_1RD_2, it varies along any direction. The behavior of the function $A^{(1)}$ in the indicated regions is considered similarly. In particular, above the weak discontinuity B_2E_2, this function is constant along the characteristics of the first family, and behind the weak discontinuity D_2H_2, it is constant along the lines $y = \text{const}$.

To this point, the solution was constructed by formal expansion of the functions in series in the small parameter of the problem. The solutions obtained by this expansion are inadequate at considerable distances from the interaction region. To prove this assertion, we write the equation for $\vartheta^{(2)}$ obtained after substitution of series (2.1) into system (1.1) and retention of terms at δ^2:

$$\frac{\partial \vartheta^{(2)}}{\partial y} + A_{w1}\,\frac{\partial \vartheta^{(2)}}{\partial x} = -\frac{\mathrm{M}_{w1}^2}{A_{w1}}\,\vartheta^{(1)} + \frac{1}{A_{w1}}\,A^{(1)}.$$

Taking into account that the right side of this equation is constant in the region considered, we obtain

$$\vartheta^{(2)} = \Big[-\frac{\mathrm{M}_{w1}^2}{A_{w1}}\,\vartheta^{(1)} + \frac{1}{A_{w1}}\,A^{(1)}\Big]\, y + \tilde f(x - A_{w1}y).$$

The presence of a secular term on the right side indicates that the expansion obtained is uniform over y.

It should be noted that the interaction region is unbounded along both y and on x. However, along x, the expansion is uniform. This follows from the fact that behind the characteristic D_2H_2, the angle ϑ is equal to zero in both the zero and first approximations, so that after integration along the streamlines, the derivatives on the left side $df/d\nu_3$ do not contain secular terms.

Taking into coconut the aforesaid, we introduce the strained coordinates s and t by the formulas

$$x - A_{w1}y = s + \delta\varphi_2(s, t) + \ldots, \qquad A_{w1}y = t.$$

Then, for the function ϑ in the first and second approximations, we obtain

$$\delta^1\colon \qquad \frac{\partial\vartheta^{(1)}}{\partial t} = 0 \quad\Longrightarrow\quad \vartheta^{(1)} = \vartheta^{(1)}(s),$$

$$\delta^2\colon \qquad \frac{\partial\vartheta^{(2)}}{\partial t} - \frac{\partial\vartheta^{(1)}}{\partial s}\,\frac{1}{A_{w1}}\Big[A_{w1}\,\frac{\partial\varphi_2}{\partial t} + \vartheta^{(1)}\mathrm{M}_{w1}^2 - A^{(1)}\Big] = 0.$$

Choosing $\varphi_2(s,t)$ from condition

$$A_{w1}\,\frac{\partial\varphi_2}{\partial t} = -\vartheta^{(1)}\mathrm{M}_{w1}^2 + A^{(1)}$$

so that

$$\varphi_2 = f(s) - \frac{1}{A_{w1}}\int\limits_0^t [\vartheta^{(1)}\mathrm{M}_{w1}^2 - A^{(1)}]\,dt, \tag{4.2}$$

we have

$$\frac{\partial\vartheta^{(2)}}{\partial t} = 0 \quad\Longrightarrow\quad \vartheta^{(2)} = \vartheta^{(2)}(s).$$

As noted above, behind the streamline B_2E_2 the functions $\vartheta^{(1)}$ and $A^{(1)}$ do not vary along the characteristics of the first family, i.e., they depend only on the variable s. Designating

$$g(s) := \frac{1}{A_{w1}}\int\limits_0^{t_0}\Big[\vartheta^{(1)}\mathrm{M}_{w1}^2 - A^{(1)}\Big]\,dt,$$

where t_0 is the value of t on the streamline B_2E_2, we choose the function $f(s)$ in formula (4.2) such that $f(s) = g(s)$. With this choice of $f(s)$, the function $\varphi(s)$ above the line B_2E_2 is equal to

$$\varphi(s) = \Phi(s)(t-t_0), \qquad \Phi(s) = \frac{A^{(1)}(s) - \vartheta^{(1)}(s)\mathrm{M}_{w1}^2}{A_{w1}} = \frac{\mathrm{M}_{w1}^2F_1^{(1)}(s)}{2(1+\varepsilon)A_{w1}^3}$$

and the relationship between the new and old variables takes the form

$$y = t/A_{w1}, \qquad x = t + s + \delta\Phi(s)(t-t_0). \tag{4.3}$$

5. Formation of a Shock in the Wave Reflected from the Wall. Under particular vorticity distributions, the reflected wave $F_1C_1B_2D_2$ can be a compression wave. The reflection from the wall does not change the type of wave, so that the reflected wave $C_1H_1D_2H_2$ is also a compression wave. In this case, at a distance from the wall of about $1/\delta$, the neighboring characteristics of the first family intersect and a shock is formed in the flow. At the point of intersection of the characteristics, the Jacobian of the map (4.3) is equal to zero. Using (4.3), it is easy to obtain the condition of equality of the Jacobian to zero:

$$t = t_0 - \frac{2(1+\varepsilon)A_{w1}^3}{\delta\mathrm{M}_{w1}^2F_1'(s)} = t_0 - \frac{2(1+\varepsilon)A_{w1}^3}{\delta\mathrm{M}_{w1}^2P_1^{(1)}(s)}. \tag{5.1}$$

On the plane (s,t), relation (5.1) specifies a certain curve $t = t_d(s)$ (curve 1 in Fig. 6), whose shape is defined by the function $P_1^{(1)}(s)$. The last function is continuous, and in the region $[s_1, s_2]$ bounded by the characteristics C_1H_1 and D_2H_2, it is different from zero. Hence, these characteristics are oblique asymptotes for the curve of $t_d(s)$. If the function $P_1^{(1)}(s)$ has roots at the interior points of the interval (s_1, s_2), then the curve of $t_d(s)$ has several branches separated by oblique asymptotes parallel to C_1H_1 and D_2H_2. We are interested only in the parts of the curve that lie in the half-plane $t > 0$, i.e., the intervals of variation of s for which $P_1^{(1)}(s) < 0$. On these intervals, the global maximum points of the function $P_1^{(1)}(s)$ correspond to the points of the curve the least distant from the wall. At these points, there is origin of the shock.

We assume that in the neighborhood of one of such points — the point (s_c, t_c) — the function $P_1^{(1)}(s) \in C^1$ and has a second derivative. Let us show that in the neighborhood (s_c, t_c), the curve $t_d(s)$ has the shape of a semicubic parabola. Indeed, locally,

$$\Phi(s) = \Phi(s_c) + \Phi'(s)(s-s_c) + \Phi'''(s)(s-s_c)^3/6.$$

We substitute this expression into (4.3):

$$x = t + s + \delta(t-t_0)(\Phi(s_c) + \Phi'(s)(s-s_c) + \Phi'''(s)(s-s_c)^3/6). \tag{5.2}$$

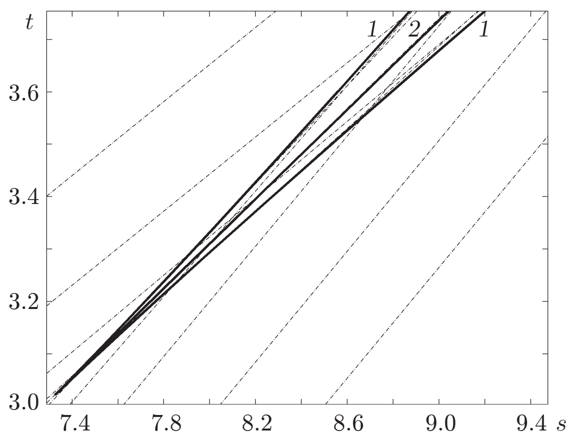

Fig. 6. Formation of a shock in the wave reflected from the wall.

On the plane (x,t), the last equality specifies a family of straight lines that depend on s as on a parameter. The equation of the envelope of this family can be obtained by differentiating (5.2) with respect to s:

$$0 = 1 + \delta(t - t_0)(\Phi'(s) + \Phi'''(s)(s - s_c)^2/2). \tag{5.3}$$

Excluding the parameter s from system (5.2), (5.3), we obtain the desired equation of the envelope. In this system, we convert to new variables:

$$t_* = t - t_0 + 1/(\delta\Phi'(s_c)), \qquad x_* = x - t - s_c - \delta\Phi(s_c)(t - t_0), \qquad s_* = s - s_c.$$

In these variables, the system becomes

$$t_* = \frac{cs_*^2}{b(b + cs_*^2)}, \qquad x_* = \frac{2}{3}\,bt_*s_*, \qquad b = \delta\Phi'(s_c), \quad c = \frac{1}{2}\,\delta\Phi'''(s_c).$$

For small s_*, the last equalities can be written as

$$t_* = \frac{c}{b^2}\,s_*^2 + O(s_*^4), \qquad x_* = \frac{1}{3}\,\frac{\Phi'''(s_c)}{\Phi'(s_c)}\,s_*^3 + O(s_*^5).$$

Hence, in the neighborhood of the maximum point, the envelope of the family of straight lines indeed has the shape of a semicubic parabola.

We now construct a function $g(t)$ that describes the shape of the shock (curve 2 in Fig. 6). At any point of the shock with the coordinates $(t, g(t))$, equalities (4.3) are valid. Hence,

$$g(t) = t + s_1 + \delta\Phi(s_1)(t - t_0) = t + s_2 + \delta\Phi(s_2)(t - t_0). \tag{5.4}$$

Here s_1 and s_2 are the values of the parameter s on the sides of the discontinuity. It is easy to show that in the case of a weak discontinuity, the slope σ of the shock to the incoming flow streamline is linked to the angle β of flow rotation at the shock and to slopes $\alpha_{1.2}$ of the characteristics in the flow ahead of and behind the shock by the relation

$$\cot\,\sigma = (\cot\,\alpha_1 + \cot\,(\alpha_2 + \beta))/2 = (A_1 + \cot\,(\alpha_2 + \beta))/2.$$

Indeed, it is possible to show that

$$\cot\,\sigma = A_1 - \frac{A_1^2 + 1}{2(1+\varepsilon)A_1}\,z + \frac{(A_1^2 + 1)(3A_1^2 - 1)}{8(1+\varepsilon)^2 A_1^3}\,z^2 + O(z^3), \qquad z \to 1,$$

$$\cot\,(\alpha_2 + \beta) = A_1 - \frac{A_1^2 + 1}{(1+\varepsilon)A_1}\,z + \frac{(A_1^2 + 1)(3A_1^2 - 1)}{2(1+\varepsilon)^2 A_1^3}\,z^2 + O(z^3), \qquad z \to 1.$$

Hence, with accuracy to terms of the second order in z, the shock bisects the angle between the characteristics:

$$\frac{dg(t)}{dt} = \frac{1}{2}\Big[\frac{dx(s_1)}{dt} + \frac{dx(s_2)}{dt}\Big] = 1 + \frac{\delta}{2}\,[\Phi(s_1) + \Phi(s_2)]. \tag{5.5}$$

Relations (5.4) and (5.5) allow us to determine the desired functions $g(t)$, $s_1(t)$, and $s_2(t)$ [20]. Indeed, we differentiate (5.4) wit respect to t and equate the expressions obtained and (5.5):

$$\frac{dg(t)}{dt} = 1 + \frac{\delta}{2}\,[\Phi(s_1) + \Phi(s_2)] = 1 + s_1'(t) + \delta\Phi(s_1) + \delta\Phi'(s_1)s_1'(t)(t - t_0)$$

$$= 1 + s_2'(t) + \delta\Phi(s_2) + \delta\Phi'(s_2)s_2'(t)(t - t_0).$$

For conservation of symmetry, we take the arithmetical mean of the last two expressions and eliminate $t - t_0$ from them using the following relation resulting from (5.4)

$$t - t_0 = -\frac{s_2 - s_1}{\delta(\Phi(s_2) - \Phi(s_1))}. \qquad (5.6)$$

As a result, we obtain the equality

$$(s_1' + s_2')(\Phi(s_2) - \Phi(s_1)) = (s_2 - s_1)(\Phi'(s_1)s_1' + \Phi'(s_2)s_2'),$$

which can be written as

$$\frac{s_2 - s_1}{2}\,(\Phi(s_2) + \Phi(s_1)) = \int\limits_{s_1}^{s_2} \Phi(s)\,ds = G(s_2) - G(s_1), \qquad G(s) = \int\limits_{s_{\min}}^{s} \Phi(s)\,ds. \qquad (5.7)$$

From formula (5.7) we can find $s_2 = s_2(s_1)$ and then, using (5.6), the desired function $g(t)$.

The authors thank V. R. Meshkov for useful discussions and help in numerical calculations.

REFERENCES

1. A. E. Medvedev and V. M. Fomin, "Approximate analytical calculation of the Mach configuration of steady-shock waves in a flat convergent channel," *J. Appl. Mech. Tech. Phys.*, **39**, No. 3, 369–375 (1998).
2. A. V. Omel'chenko, V. N. Uskov, and M. V. Chernyshev, "One approximate analytical model for the flow in the first roll of an overdriven jet," *Pis'ma Zh. Tekh. Fiz.*, **29**, No. 6, 56–62 (2003).
3. H. Li and G. Ben-Dor, "Oblique shock-expansion fan interaction — analytical solution," *AIAA J.*, **34**, No. 2, 418–421 (1996).
4. V. R. Mehskov, A. V. Omle'chenko, and V. N. Uskov, "Interaction of a shock with a counterpropagating rarefaction wave," *Vest. S.-Peterb. Univ.*, Ser. 1, No. 2 (No. 9), 99–106 (2002).
5. W. D. Hayes and R. F. Probstein, *Theory of Hypersonic Flows*, Academic Press, New York (1959).
6. G. G. Chernyi, *Gas Flows with a High Supersonic Velocity* [in Russian], Fizmatgiz., Moscow (1959).
7. L. V. Ovsyannikov, *Lectures on the Fundamentals of Gas Dynamics* [in Russian], Nauka, Moscow (1981).
8. L. V. Ovsiannikov, *Group Analysis of Differential Equations*, Academic Press, New York (1982).
9. P. Olver, *Applications of Lie Groups to Differential Equations*, Springer Verlag (1993).
10. M. Van Dyke, *Perturbation Methods in Fluid Mechanics*, Parabolic Press, Stanford (1975).
11. A. H. Nayfeh, *Perturbation Methods*, Wiley, New York (1973).
12. M. J. Lighthill, "A technique for rendering approximate solutions to physical problems uniformly valid," *Phil. Mag.*, No. 40, 1179–1201 (1949).
13. M. J. Lighthill, "The shock strength in supersonic 'conocal fields'," *ibid.*, pp. 1202–1223.
14. M. J. Lighthill, "A technique for rendering approximate solutions to physical problems uniformly valid," *Z. Flugwiss.*, No. 9, 267–275 (1961).
15. G. B. Witham, "The flow pattern of a supersonic projectile," *Comm. Pure Appl. Math.*, No. 5, 301–348 (1952).
16. G. B. Witham, "The propagation of weak spherical shocks in stars," *Comm. Pure Appl. Math.*, No. 6, 397–414 (1953).
17. C. C. Lin, "On a perturbation theory based on the method of characteristics," *J. Math. Phys.*, No. 33, 117–134 (1954).
18. P. A. Fox, "Perturbation theory of wave propagation based on the method of characteristics," *J. Math. Phys.*, No. 34, 133–151 (1955).
19. B. L. Rozhdestvenskii and N. N. Yanenko, *Systems of Quasilinear Equations and Their Applications to Gas Dynamics* [in Russian], Nauka, Moscow (1968).
20. J. Whitham, *Linear and Nonlinear Waves*, Wiley, New York (1974).